Remote Sensing-Based Assessment of Mangrove Ecosystem with Special Reference to the Sundarbans of India

Dhananjay Barman, Sanjeev Kumar Srivastava, Gouranga Kar, Saon Banerjee, Debangana Banik, Bulu Basak, Mohammed A. S. Arfin-Khan, Sharif A. Mukul, Mochamad Candra Wirawan Arief, and Reginawanti Hindersah

Abstract Mangrove forests are unique ecosystems that exist on tropical and subtropical coastal wetlands throughout the world. They provide multiple ecosystem services which are ecologically and economically beneficial to the planet by providing food and fodder, fish and shrimp breeding, protection from cyclones, coastal erosion, and saltwater intrusion, providing medicinal ingredients, and attracting tourists. However, these mangrove ecosystems face multiple facets of climatic, ecological, and anthropogenic threats of extinction. The area under mangrove forest has drastically reduced over the time. For the protection and conservation of the mangrove forests, there is an urgent need for accurate mapping of mangrove area and assessment of their vulnerability to climate change, and other abiotic, biotic, and

D. Barman (✉) · G. Kar · D. Banik · B. Basak
ICAR—Central Research Institute for Jute and Allied Fibres, Kolkata, West Bengal, India

S. K. Srivastava
Geospatial Analytics for Conservation and Management, School of Science Technology and Engineering (SSTE), Sippy Downs, QLD, Australia

S. Banerjee
Bidhan Chandra Krishi Viswavidyalaya, Mohanpur, India

M. A. S. Arfin-Khan
Department of Forestry and Environmental Science School of Agriculture and Mineral Sciences, Shahjalal University of Science and Technology, Sylhet, Bangladesh

S. A. Mukul
United International University, Dhaka, Bangladesh

M. C. W. Arief
Center for Environment and Sustainability Science, Faculty of Fishery and Marine Science, Universitas Padjadjaran, Sumedang, West Java, Indonesia

R. Hindersah
Center for Environment and Sustainability Science, Faculty of Fishery and Marine Science, Universitas Padjadjaran, Sumedang, West Java, Indonesia

Faculty of Agriculture, Universitas Padjadjaran, Sumedang, West Java, Indonesia

© The Author(s), under exclusive license to Springer Nature Switzerland AG 2026

S. K. Srivastava et al. (eds.), *Earth Observation for Monitoring Mangrove Ecosystems*, https://doi.org/10.1007/978-3-032-16668-5_5

anthropogenic threats. The remote sensing technique can play a vital role in assessing and providing spatiotemporal information on mangrove ecosystem distribution, species differentiation, health status, and ongoing changes of mangrove cover. Due to difficulty in accessing the mangrove areas by humans, various studies have been conducted by using different remote sensing techniques ranging from aerial photography to high- and medium-resolution optical imagery and from hyperspectral data to active microwave (SAR) data. Numerous scientific papers have reported studies on mangrove mapping, distribution, and health status over the last few decades. This chapter will primarily present how remote sensing techniques have been utilized by various researchers to address the multiple factors related to mangrove studies, including the Sundarbans mangrove of India, which is a UNESCO World Heritage site.

Keywords Mangrove forest · Remote sensing of mangrove · Coastal ecosystem mapping · Reflectance and backscattering properties of mangroves · Disaster mapping for mangrove

1 Introduction

Mangrove forests exist on tropical and subtropical coastal wetlands throughout the world (Chapman, 1976; Tomlinson, 2016). They are among the most biologically important ecosystems on the planet. Mangrove forests consist of trees, shrubs, and fern species (Duke et al., 1998) that have adapted to the harsh conditions of high salinity, anoxic soils, warm air and water temperatures, high tides, and muddy waters. These ecosystems act as a first line of defence against tropical and subtropical cyclones, hurricanes, and tsunamis by dissipating wave and wind energy. Moreover, the mangrove ecosystems provide tremendous ecological and economic services to mankind by providing food, fodder, fuel, medicine, recreation, etc. This also helps to regulate the environment by absorbing atmospheric carbon di-oxide, stabilizing coastlines, and protecting against storms. According to Barbier et al. (2011), the benefits from carbon sequestration depend on factors like the density of their biomass and the price of carbon in the market which can vary extensively ranging from around $60 to more than $1000 per hectare each year. Additionally, the storm protection it offers has been valued from $300 to as high as $9000 per hectare annually. In the Sundarbans, research showed that local communities gain substantial economic benefits from mangroves and are open to investing in their conservation. For instance, Iqbal (2020) used a choice experiment approach to estimate the marginal willingness to pay (MWTP) for improvements in ecosystem services. Also, Mukherjee et al. (2014) emphasized light on the ecological and economic trade-offs in the mangrove forests of South Asia, underscoring the importance of integrated valuation in policymaking and land-use planning. Even though there are obstacles like hypothetical bias, limited data, and challenges in capturing cultural

services, these valuation efforts play a vital role in shaping Payment for Ecosystem Services (PES) initiatives, blue carbon strategies, and adaptive climate policies.

However, these mangrove ecosystems face multi-facets of climatological, ecological, and anthropogenic threats of extinction. Many parts of the ecosystems have immersed into sea water because of the sea-level rise due to global warming. The regeneration capacity of mangroves has been overtaken by the more frequent cyclonic events. Many parts of the mangrove forests have been degraded polluted and have lost biodiversity. Biodiversity in mangrove forests is increasingly at risk. In estimation, 1533 species are associated with mangroves, 15% of which are threatened with extinction. UNEP's report 'Decades of Mangrove Forest Change: What does it mean for nature, people and the climate?' found that nearly 50% of mangrove-associated mammals, 22% of fishes, 16% of plants, 13% of amphibians, and 8% of bird and reptile species are threatened with extinction. Worryingly, for 44% of the species, their extinction risk is increasing and of those already at risk, the situation is getting worse for 89%.

For addressing these issues and challenges, a proper and systematic assessment of the mangrove ecosystems is essential. As the manual survey and assessment is very difficult, and in some places, it is almost impossible due to the rough and tough characteristics of the ecosystems, satellite and unmanned aerial vehicle (UAV) can play a vital role in assessing the mangrove ecosystem. Many researchers worldwide have applied these techniques to assess the health of the mangrove ecosystem. These techniques in combination with modern-day artificial intelligence (AI) and machine learning (ML) techniques can provide even more real-time data in framing better management strategies for the mangrove ecosystems.

2 Global Distribution and Current State of the Mangrove Ecosystem

The global area of mangrove forest has been estimated to 147,359 km^2 (Global Mangrove Watch, 2020), 51% of which occurred in the Asia-Pacific, with 29% in the Americas, and 20% in Africa. Over the 24-year period from 1996 to 2020, it has been reported that the global mangrove forest cover has lost in the extent of 5245 km^2 (3.4%). However, in a latest assessment of UNEP using current satellite imagery, the global loss of mangroves has stabilized, and the mangrove cover increased in and around world's large rivers, estuaries, and deltas (UNEP, 2023).

According to the Global Forest Resource Assessment 2020 (FRA, 2020), 113 nations throughout the world have mangrove forests covering an estimated 14.72 million hectares. Asia has the highest documented mangrove area (5.33 million hectares), followed by South America (2.12 million hectares), Western and Central Africa (2.30 million hectares), North and Central America (2.55 million hectares), and Oceania that is claimed to have the least area of mangroves (1.26 million hectares). As per FRA 2020 report (Table 1), the global mangrove-cover between 1990 and 2020 declined from 15,759 hectares (157,590 km^2) to 14,717 hectares (147,170 km^2). Asia experienced the most significant loss, particularly in South and Southeast Asia (12.9%), where factors such as urbanization, aquaculture, and

Table 1 Global status of the mangrove cover

Region/subregion	Mangrove area (1000 ha)			
	1990	2000	2010	2020
Eastern and Southern Africa	929	902	883	905
Northern Africa	34	31	32	31
Western and Central Africa	2436	2400	2349	2304
Total Africa	3398	3332	3264	3240
East Asia	24	22	25	32
South and Southeast Asia	6117	6108	5713	5330
Western and Central Asia	190	190	190	184
Total Asia	6331	6320	5928	5545
Total Europe	0	0	0	0
Caribbean	787	789	774	891
Central America	492	482	483	466
North America	1152	1167	1190	1195
Total North and Central America	2431	2439	2447	2552
Total Oceania	1447	1150	1314	1255
Total South America	2152	2050	1976	2124
World	**15,759**	**15,292**	**14,928**	**14,717**

Source: FRA (2020), FAO

coastal development contributed to a loss of nearly 800 thousand hectares. Africa experienced a mild decrease, particularly in its western and central areas (4.6%), while Eastern and Southern Africa started to show a bit of recovery by 2020. Oceania, on the other hand, faced a net loss of 13.7%, even though there was some improvement noted in 2010. However, according to FSI Report 2023, India ranks as the world's third richest nation in terms of mangrove plant diversity, trailing behind Indonesia and Australia. More than 40% of the total area of mangroves was found to be in only four countries: Indonesia (19%), Brazil (9%), Nigeria (7%), and Mexico (6%). The status of world mangrove cover in 2024 shows that Southeast Asia has the largest share of mangrove cover, making up 33.6% of the total cover, followed by North and Central America and the Caribbean (14.4%), South America (13.2%), and West and Central Africa (15.5%). East and Southern Africa (5.3%), South Asia (6.6%), and Australia and New Zealand (7.0%) are other regions with moderate coverage. On the other hand, mangrove cover is comparatively low in the Pacific Islands (3.9%), the Middle East (0.2%), and East Asia (0.2%) (Fig. 1).

3 Climatic Variability of Mangrove Ecosystems

Climate change and its variability can significantly impact on mangrove ecosystems, which depend on species sensitivity and location (Randhir et al., 2024; Ward et al., 2016). Changes in temperature and rainfall due to climate change affect growth and development stages of mangrove species, leading to variations in leaf

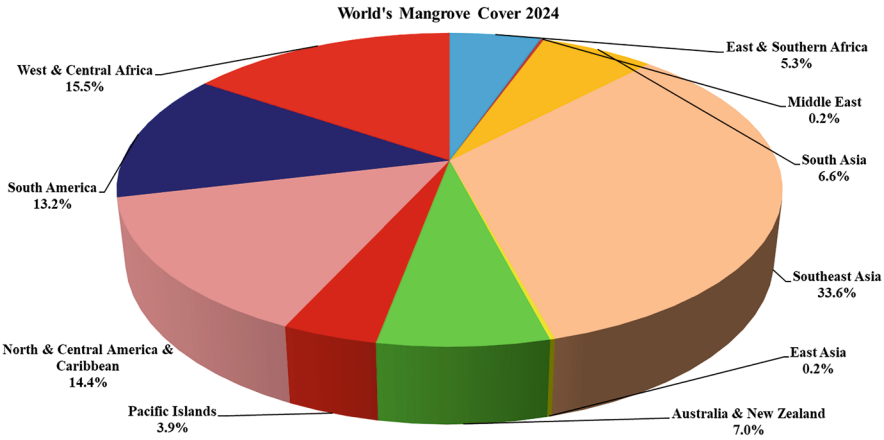

Fig. 1 The current status of the world's mangrove cover. [*Source*: The State of the World's Mangroves 2024]

area index (LAI) resulting changes in remotely sensed indices (e.g. Normalized Difference Vegetation Index, NDVI; Enhanced Vegetation Index, EVI) if data is not captured during peak biomass (Ganguly et al., 2012). Climate-driven shifts in species composition and structure alter spectral reflectance, reducing the accuracy of biomass models based on historical data (Clark et al., 2003). In tropical regions like the Sundarbans, increased cloud cover and atmospheric disturbances degrade optical sensor data quality, thus making it difficult for monitoring and assessment of the mangrove ecosystem (Baccini et al., 2017). The effects of climate change on three dominant mangrove species globally: red, black, and white mangroves, were studied using simulation, GIS, and statistical modelling and revealed that low precipitation can impact growth of all three mangrove species, where even 1 mm reduction in precipitation decreased the growth suitability of red, black, and white mangroves by 0.008%, 0.004%, and 0.008%, respectively (Randhir et al., 2024).The Intergovernmental Panel on Climate Change (IPCC) in 2013 reported that the global sea levels are likely to rise by between 0.28 and 0.98 m by 2100 which will cause coastal flooding in future. In recent decades, global sea-level rise has been reported at the rate of 3.2 ± 0.4 mm per year (Church & White, 2011). However, regional factors influence its variability from 1.9 mm per year in the Caribbean to 7.5 mm per year in parts of Indonesia (Nerem et al., 2010) and up to 9 mm per year in the lower Mississippi River Delta (NOAA, 2015). Sea-level rise can cause harm to mangrove by increasing inundation duration which leads to plant death (He et al., 2007) and shifting in species composition (Gilman et al., 2008). Sea-level rise and associated danger of sinking of mangrove area should be monitored periodically by using remote sensing (RS) data for taking appropriate climate action. Keeping in view the importance of the climate, an account of climatic situation of the major mangrove regions is presented in the Table 2.

Table 2 Climate of the mangrove regions of different countries of the world

Country	Area (in ha)	% global total	Rainfall (mm)	Temperature range (°C)	RH (%)	Tidal influence (m)
Indonesia	3,112,989	22.6	2000–4000	25–30	≥80	Semi-diurnal (1–3)
Australia	977,975	7.1	1000–3500	24–30	≥70	Intertidal (2–4)
Brazil	962,683	7.0	1500–2500	25–30	≥80	Semi-diurnal (2–4 and ≥4)
Mexico	741,917	5.4	1000–2500	25–30	≥80	Semi-diurnal (1–2 and ≥3)
Nigeria	653,669	4.7	1500–3000	26–30	≥80	Semi-diurnal (1–2)
Malaysia	505,386	3.7	2000–4000	25–32	≥80	Semi-diurnal (1–3)
Burma (Myanmar)	494,584	3.6	1500–5000	25–32	≥80	Semi-diurnal (2–4)
Papua new Guinea	48,121	3.5	2000–3500	26–30	≥80	Semi-diurnal (1.5–4)
Bangladesh	436,570	3.2	1500–3000	24–32	≥80	Semi-diurnal (3–6)
Cuba	421,538	3.1	1000–1500	24–30	≥80	Semi-diurnal (0.5–1.5)
India	368,276	2.7	1500–3000	25–32	75–85	Diurnal and semi-diurnal (2–6)
Guinea Bissau	338,652	2.5	1200–2000	25–32	70–80	Semi-diurnal (2–3)
Mozambique	318,652	2.3	1000–1500	25–30	70–80	Intertidal (1.5–3)
Madagascar	278,078	2.0	800–1500	25–30	≥80	Semi-diurnal (1.5–4)
Philippines	263,137	1.9	1500–3000	25–32	80–90	Intertidal (1–2)

4 Mangrove Area Mapping and Classification

The integration of satellite imagery with geospatial analysis has significantly improved the ability of researchers to detect changes in mangrove cover, evaluate species distribution, identify areas under ecological stresses, and distinguish mangroves from adjacent land cover types such as agricultural fields, mudflats, and inland vegetation (Kuenzer et al., 2011). Challenges in mangrove classification arose due to similar reflectance from other vegetation, rice fields, and water bodies. To overcome this, masking techniques can be used to separate mangrove areas from non-mangrove vegetation and water bodies, thus improving the accuracy of the classification (Salam et al., 2007). The unsupervised classification using 30 clusters in a study yielded an overall accuracy of 78.32% while supervised classification,

supported by 272 ground-truth points, performed better with 81.62% accuracy. In the former method, the water bodies were classified accurately, but misclassifications occurred in identifying species like Gewa and grassland/bare land areas. Some of the classification errors in both methods could be attributed to environmental differences and a time gap between the acquisition of the satellite images and the creation of the mangrove inventory map. Despite this, both methods were considered reliable, with supervised classification slightly outperforming the unsupervised approach. However, some researchers reported that the use of machine learning algorithms such as Support Vector Machines (SVMs) and Random Forest (RF) has even been better to classify mangrove species and mapping and monitoring of mangrove forests (Campomanes et al., 2016; Jiang et al., 2021). The overall accuracy of RF can be 99.17%, whereas SVM showed 95.83% accuracy. Thus, these algorithms can be used for mapping and classification of mangrove ecosystems all over the world.

Numerous researchers used remote sensing techniques for mapping of Indian Sundarbans region (Biswas et al., 2024; Mondal & Bandyopadhyay, 2014; Mitra & Karmaker, 2010; Giri et al., 2007). Net erosion of approximately 3.7 km^2 per year across the Indian Sundarbans Delta between 1980 and 2021, with 243 km^2 of erosion and 91 km^2 of accretion over a 41-year period, was estimated using the NDVI (Biswas et al., 2024). Ghosh et al. (2015) employed an unsupervised (ISODATA) classification on a multi-temporal and multiscale analysis mapping colonial-era charts alongside 1960s Corona imagery and Landsat satellite data and found that the overall mangrove area in the Indian Sundarbans system remained relatively constant over time and there were significant internal changes in forest condition and stand structure, reflecting shifts in density and health of mangrove species. Giri et al. (2007) conducted a multi-temporal Landsat analysis from the 1970s to 2000s and reported that mangrove forest area in the Sundarbans decreased by approximately 1.2% over that period, with a more pronounced decline of approximately 2.5% between 1990s and 2000s. In another study, Datta and Deb (2012) employed multi-temporal Landsat data to investigate on land use/land cover (LULC) changes between 1975 and 2006 revealing a substantial decline of around 0.42% of the area's initial mangrove cover, primarily in the Sundarbans' forest-habitation interference zones. Kundu et al. (2021) classified Landsat imagery using NDVI from 1975 to 2018 into dense forest, sparse forest, water bodies, and wetland and found a net loss of approximately 2.1% ($\approx$ 47 km^2) of forest area, with varying trends in fragmentation and density. Mondal et al. (2018) used Landsat MSS and OLI multispectral satellite imagery to classify land use/land cover (LULC) on Sagar Island into categories such as forest vegetation, agriculture, built-up area, water bodies, and wetlands. Their classification achieved an overall accuracy of 79.53%, with a Kappa coefficient (K) of 0.7465.

4.1 Change Detection of Mangrove

The decrease in mangrove cover and its density is a threat to its flora and fauna. The monitoring of change in mangrove cover can be performed by adapting various change detection methods of the remote sensing (RS) technique. The traditional change detection methods like post-classification comparison (PCC), unsupervised conventional change detection, change vector analysis (CVA), and single threshold algorithm (STA) had limitations. To overcome this, Shimu et al. (2019) proposed a new method of using the Normalized Difference Vegetation Index (NDVI) to track changes in vegetation over a temporal scale, resulting in both progressive and regressive changes in mangrove vegetation.

The land use/land cover (LULC) change study in the South-Western Indian Sundarbans Biosphere Reserve from 1975 to 2006 using Landsat imagery showed a significant loss of open mangrove areas and biodiversity, particularly in forest--habitation zones, while dense mangrove cover increased in the reserved forests, indicating effective management (Datta & Deb, 2012). The study also showed that overall, the region lost about 0.42% of its original mangrove cover, and the rise of nonagricultural lands is linked to the growth of settlements, tourism, and alternative livelihoods like shrimp farming and commercial fishing, although harmful practices like prawn seed collection persisted.

Recent advances in remote sensing technologies have greatly improved LULC change mapping, particularly for mangrove ecosystems. High-resolution satellite images from sensors such as Sentinel and Landsat have enabled precise and accurate mapping of changes in mangrove cover over time (Kuenzer et al., 2011; Parida & Kumar, 2020). Samanta and Hazra (2016) employed a hybrid classification approach using Landsat TM/ETM+ imagery from 1986, 1996, 2002, and 2012 to assess mangrove cover changes in the Indian Sundarbans. By using the hybrid approach in combination of unsupervised (ISODATA) and supervised (Maximum Likelihood Classifier) classification techniques, they were able to classify the mangrove area into six land cover classes like dense forest, degraded forest, saline blanks, water body, sand (beaches/dunes), and mud flats. They obtained the classification accuracies between 85 and 90% and Kappa values of 0.79–0.88. Changes were analysed using post-classification comparison, highlighting spatial and temporal patterns of mangrove degradation and conversion, particularly in forest–habitation interference zones. Kumar et al. (2019) used five vegetation indices, viz. Mangrove Probability Vegetation Index (MPVI), Normalized Difference Wetland Vegetation Index (NDWVI), Shortwave Infrared Absorption Depth (SIAD), Normalized Difference Infrared Index (NDII) and Atmospherically Resistant Vegetation Index (ARVI) in the decision tree algorithm to improve the separability of mangrove forests from adjacent land cover classes, especially terrestrial vegetation using Support Vector Machine (SVM), Minimum Distance (MD), and Spectral Angle Mapper (SAM) and found that SVM performed better than MD and SAM with an overall precision of 99.08%over the Indian Sundarbans.

The impact analysis of LULC changes is essential for prioritizing the management practices. Thakur et al. (2021) analysed the impact of LULC changes in the Indian Sundarbans from 2000, 2010, and 2017, using Landsat TM, ETM+, and OLI imagery, and found a decline in mangrove swamps, plantations, and agricultural land, while sand beaches, mudflats, rivers, and agriculture increased. NDVI values dropped for mangroves from 0.441 to 0.229 and plantations from 0.266 to 0.195 but rose for rivers and aquaculture. Land Surface Temperature (LST) increased in settlements and sand beaches, showing a negative correlation with NDVI, likely due to the high evapotranspiration of mangroves. The results indicated the growth of non--vegetated areas and ecosystem stress. Similar results were reported by Kanjin and Alam (2024) where they showed changes in mangrove coverage from 1973 to 2023 using Landsat (Landsat 1–8) data and examined the relationship between vegetation health with NDVI and surface temperature using Moderate Resolution Imaging Spectroradiometer (MODIS) data in Bangladesh and Indian Sundarbans. Despite mangrove loss, vegetation health improved, indicating resilience. The study found a weak negative correlation between NDVI and LST, suggesting other factors, such as water bodies and land cover heterogeneity, also influenced temperature. The findings highlighted the need for conservation to prevent further degradation.

4.2 Disaster Mapping in Mangrove

Disasters are increasingly threatening populations and affecting sustainable development in the mangrove region. Satellite and unmanned aerial vehicle (UAV) technologies play a key role in disaster management by aiding in preparedness, warning, and response. However, challenges like limited access to high-resolution data and technological gaps remain, particularly between developed and developing countries. Recent advancements, including new spatiotemporal data sources and improved resolutions, offer different kind of solutions (Bello & Aina, 2014). SERVIR-Mekong initiative, in collaboration with NASA and USAID, is one such effort for disaster management carried out with the help of the Asian Disaster Preparedness Center and various regional partners in Cambodia, Laos, Thailand, Myanmar, and Vietnam (SERVIR Global, 2023). It plays a crucial role by offering free access to satellite data, dashboards, and customized decision-support tools designed for flood mapping, early warning systems, and monitoring of the mangrove ecosystem. By linking global data resources with local engagement and training, this showcases how countries can work together to fill gaps in data and capacity. This type of initiative empowers vulnerable coastal communities to manage disaster risks more effectively and boost their environmental resilience (SEI, 2023).

The entire global mangrove ecosystems, including the Indian Sundarbans, are exposed to various disasters like cyclones, hurricanes, typhoons, tsunamis and storm surges, flood inundation, embankment breaching, and coastal erosion (IUCN, 2025; Ghosh & Mistri, 2022). These disasters result severe ecological damage, which can be estimated by using Moderate Resolution Imaging Spectroradiometer

(MODIS) Global Disturbance Index (MGDI) given by Mildrexler et al. in 2009. For monitoring and management of cyclonic disasters, the MGDI was used by Dutta et al. (2015) in the Indian Sundarbans and found that the mangrove landmass decreased by approximately 329.45 km^2 at a rate of 7.48 km^2 per year from 1973 to 2017. Mandal et al. (2022) implemented the Analytic Hierarchy Process (AHP) along with Random Forest (RF) and Artificial Neural Network (ANN) to map multi--hazard risk of the Sundarbans. Their results showed that the southern and eastern parts of the study area faced high to extremely high risk, primarily driven by cyclonic hazards and embankment breaching.

5 Degradation and Deforestation of Mangroves

The degradation of mangroves is caused by multiple factors such as sea-level rise, development of fisheries, hyper-salinity, sediment movement, storm effects, shoreline erosion, and expansion of eutrophication in the surface depressions of swampy areas (Paul et al., 2017). About 40% of the tropical and 10.5% of the Sundarbans mangroves have been lost due to induced sea-level rise, extreme weather events, and human interferences (Padhy et al., 2022; Ghosh et al., 2015). Anthropogenic factors influencing the ecosystem have indicated that human-wildlife conflict (24.4%) was considered the biggest threat, followed by climate change (19.9%), salinity change (18.8%), livelihood pressures on natural resources (16.6%), shrimp seed collection (11.5%), and environment and water pollution (8.8%) (Vyas & Sengupta, 2012).

Integrating spectral data with other spatial datasets can improve insights, and documenting the accuracy of the results helps users assess the reliability of the findings (Coops et al., 2006). Landsat satellite data, particularly the Tasseled Cap (TC) transformation, is widely used for detecting forest disturbances. This study tested four TC-based data structures, such as brightness, greenness, wetness, and a novel Disturbance Index (DI), to identify stand-replacing disturbances in Russia and Washington State, USA. The TC transformations generally outperformed the original Landsat reflectance data in detecting changes. DI performed best where disturbances are more persistent than the areas where disturbances are more transient. The study highlights that both local forest recovery rates and the time interval between Landsat acquisitions should be considered when selecting a Tasseled Cap (TC) transformation for effective disturbance detection (Healey et al., 2005).

The MODIS Global Disturbance Index (MGDI) algorithm, which uses Aqua/MODIS data (LST and EVI), maps large-scale ecosystem disturbances (LSEDs) and their impact on the global carbon cycle. The algorithm detects changes in land-surface energy by analysing annual LST composites, minimizing natural variability. Applied to North America's woody ecosystems in 2005 and 2006, MGDI accurately identified wildfires, hurricane windfalls, and logging activities. The analysis found that 1.5% of North America's woody ecosystems were disturbed in 2005 and 0.5% in 2006, with results consistent with wildfire statistics (Mildrexler et al., 2009). Deforestation and forest degradation, driven by anthropogenic stress, climate

change, and land conversion, were assessed in the Shendurney Wildlife Sanctuary, Kerala, through GIS, remote sensing, fragstat methods, and NDVI to evaluate forest degradation with spatial and nonspatial data, including anthropogenic and climate data. The disturbance index, ranging from 2.5 to 7.5, was categorized into four disturbance zones, viz. low, medium, high, and very high. This analysis supported the development of forest conservation and management strategies (Jose et al., 2011). These indices and methods can be used for assessing the mangrove degradation and deforestation globally.

6 Cyclonic Hazards in Mangrove

Due to climate change, the frequency and severity of cyclonic hazards have increased in the recent past, thereby significantly damaging the mangrove forest. Rising temperatures and rising sea levels exacerbated the damage, limiting the forest's ability to regenerate and threatening environmental sustainability (Gupta, 2021). The mangrove ecology of the Sundarbans has suffered significant damage due to super cyclones such as SIDR, Rashmi, and Aila, which has been effectively estimated by Dutta et al. (2015) using the MODIS Global Disturbance Index (MGDI). They analysed the pre- and post-cyclonic changes in EVI and LST to derive cyclonic impacts on vegetation greenness and surface temperature. The derived MGDI data were also transformed into percentage changes, and they compared them to pre- and post-cyclonic events to identify the cyclonic disturbance, with a threshold of 11% change from the temporal mean to define 'disturbed pixels'. This method can be useful to identify the cyclonic hazards in the mangrove ecosystem.

Cyclonic hazards generally occur due to the wind gusts, flooding, saltwater intrusion, storm surge, etc. (NOAA, 2023). These hazards in the mangrove have been reported by numerous researchers in the recent past (Mandal & Hosaka, 2020; Prakash et al., 2023; Mondal et al., 2024). Mandal and Hosaka (2020), using the classification and regression tree (CART), supervised classification technique on Landsat images to assess NDVI changes before and after 21 cyclones during 1988–2016 in the Google Earth Engine with 86% accuracy and a kappa coefficient of 0.80. They reported that the cyclone-affected forest area ranged from 0.5% to 24.1%, with the 18 cyclones impacting less than 10%, while the cyclone Sidr (24.1%) and one in 1988 (20.4%) caused the most damage. The cyclonic wind speed showed a significant positive correlation with the forest damage. Computing NDVI and EVI indices from the Landsat imagery, Prakash et al. (2023) found that the Amphan super cyclone caused a significant shift in mangrove cover from dense to sparse (approx. 50.18 km^2). They also reported that the barren land increased by 50.37% based on Normalized Difference Bareness Index (NDBaI), the water-bodies increased by 5.20% based on Normalized Difference Water Index (NDWI), and salinity increased based on Normalized Difference Salinity Index (NDSI).

Recently, Mondal et al. (2024) generated cyclonic flood-effective zones of the Sundarbans with the flood susceptibility spectral indices such as Normalized

Difference Vegetation Index (NDVI), Modified Normalized Difference Water Index (MNDWI), Normalized Difference Moisture Index (NDMI), Normalized Difference Built-up Index (NDBI), Bare Soil Index (BSI), and Normalized Difference Turbidity Index (NDTI) using Landsat 8 Operational Land Imager, Thermal Infrared Sensor, Resourcesat, LISS-III, and AWiFS sensors data. They found that the riverine and coastal areas in the northeast and southwest of the Sundarbans were highly susceptible to floods. Among the flood susceptibility indices, the MNDWI was found to be highly and significantly correlated with Normalized Difference Flood Index (NDFI).

7 Fire Hazards in Mangroves

Mangrove forest fires, though historically rare, have been increasingly recorded globally, particularly during natural droughts such as El Niño events, which dry out litter and peat layers, and when coupled with human activities like slash-and-burn agriculture, land conversion, and waste burning (Dookie et al., 2025). Fire hazards in mangrove forests are unlikely because of regular water inundation due to two high tides in a day. The typical swampy nature of the ecosystems is also protecting it from fire hazards. Extreme heat and high winds, especially during the dry season, further exacerbate the fire risk in the forests. The man-made fires are often attributed to discarded cigarettes from fishermen and honey collectors, clearing of paths through the mangrove forest or the flames from torches used to repel bees.

Bangladesh's Sundarbans face frequent fire hazards. Between 1970 and 2024, the Bangladesh forest department and residents reported a total of 40 fire incidents in the same area. Fire incidents in Bangladesh's East Sundarbans now occur nearly every year during the dry season. In many parts of the region, the canals that connect villages to the Sundarbans have dried up, and during summer, ponds within the mangroves also dry out. This increasing dryness leaves the forests highly susceptible to fires, which can spread rapidly due to a lack of manpower in the forest department.

Similar to the Bangladesh Sundarbans, many other mangrove ecosystems of the world are vulnerable to fire hazards. Remote sensing techniques like the Normalized Burn Ratio (NBR), Burn Area Index (BAI), and Mid-Infrared Burn Index (MIRBI) use reflectance differences in MIR and NIR bands to delineate recently burned regions versus unburned vegetation (Kurbanov et al., 2022). Using multi-temporal Landsat imagery and Normalized Burn Ratio (NBR) and differenced NBR (dNBR), a study detected that over 800 hectares of mangroves in South Sumatra experienced moderate to high burn severity (dNBR values exceeding 0.3) during the 2015 El Niño-driven fire season, particularly in inland zones, which are less influenced by tidal flooding (Crowe, 2020). Also, a fuel-type map and forest fire hazard rating for swampy mangrove forests can be developed using remote sensing data like Landsat TM imagery. By integrating this data with GIS layers such as fuel type, roads, and canals, a fire hazard rating map can be created (Razali et al., 2010). Fuzzy set theory integrated with decision-making algorithms within a GIS framework can be used to

map potential forest fire risk and guide proactive fire management efforts (Vadrevu et al., 2010). However, in contrast to the Bangladesh Sundarbans, the Indian Sundarbans is clearly defined by natural boundaries, which help keep it completely free from encroachment and, thereby, protected from fire hazards. Because of the tidal fluctuations, the entire region is flooded twice daily, preventing any fire outbreaks. Also, due to the terrain, location, and diversity of species, the area is free from grazing activities.

8 Biomass Estimation

Accurate estimation of mangrove biomass is important for determining carbon stock, exploring climate mitigation potential, and directing restoration efforts in mangrove ecosystems. Simard et al. (2019) mapped the global mangrove canopy height and biomass estimate using ICESat Geoscience Laser Altimeter System (GLAS) LiDAR data and found a significant correlation between above-ground biomass (AGB) and canopy height. Using this method, the total global mangrove carbon stock (above and below-ground biomass and soil) is estimated at 5.03 Pg. Anand et al. (2020) integrated EO-1 Hyperion hyperspectral data with Bhitarkanika field data to estimate carbon stock and biomass. Ten mangrove species were classified using the SAM classifier with a Kappa value of 0.81. Between different regression models, a second-order polynomial based on EVI provided the greatest accuracy ($R^2 \approx 0.87$), followed by NDVI ($R^2 \approx 0.84$), predicting carbon stocks between 459,820 and 514,470 tonnes.

The multi-temporal Sentinel-1 and 2 data-derived variables were used by Ghosh et al. (2021) to estimate the above-ground biomass (AGB) using variables such as, Normalized Difference Vegetation Index (NDVI), Soil Adjusted Vegetation Index (SAVI), Green NDVI (GNDVI), Normalized Difference Index produced using band 4 and 5 of Sentinel-2 data (NDI45), Inverted Red-Edge Chlorophyll Index (IRCEI), Transformed Normalized Difference Vegetation Index (TNDVI), Enhanced Vegetation Index (EVI), and Two Bands Enhanced Vegetation Index (EVI2) in Bhitarkanika Wildlife Sanctuary by Random Forest (RF), Gradient Boosted Model (GBM), and Extreme Gradient Boosting (XGB) models. The best performance was achieved using an ensemble model with a reduced RMSE of 72.86 t/ha and a normalized RMSE of 11.38% which implies that ensemble machine learning techniques enhance the precision of biomass estimation in mangrove ecosystems and support improved blue carbon assessments. In 2017, Castillo et al. estimated and mapped above-ground biomass (AGB) of mangrove forests using a combination of satellite-derived predictors that included SAR backscatter coefficients (VH and VV), GLCM texture features, and vegetation indices such as NDVI and EVI from Sentinel-2. The resulting biomass maps achieved overall accuracy between 85.3 and 86.6% with RMSE values between 27.8 and 28.5 Mg/ha and correlation coefficients (r) ranging from 0.82 to 0.84, demonstrating potential for scalable blue carbon stock assessments and land-use change monitoring.

By using image processing and digital photogrammetry, a canopy height model (CHM) generated using drone-based RGB images could reliably estimate tree height, offering an efficient method for forest inventory. This approach has the potential to enhance forest management across various land tenures and forest types (Srivastava et al., 2022). UAV-based photogrammetry combined with allometric equations improved the accuracy for estimation of above-ground biomass in both natural and restored mangrove ecosystems using digital surface models (DSM) and digital terrain models (DTM) to generate canopy height models (CHMs). The mean total AGB in natural mangroves and restored mangroves was found to be 239 Mg/ha and 232 Mg/ha, respectively (Basyuni et al., 2025). Overall, these methods provide non-destructive, scalable, and economical biomass assessment techniques that are crucial for ecosystem monitoring, blue carbon accounting, and climate mitigation plans.

9 Species Discrimination in Mangrove

Accurate monitoring of mangrove species distribution is vital for assessing their health and supporting restoration efforts due to their enormous ecological and economic importance. Hyperspectral sensors could aid species identification, though field challenges may arise (Vaiphasa et al., 2005). Spectral data (2151 bands between 350 and 2500 nm) of crown canopy leaves from 16 Thai mangrove species were captured under laboratory conditions and tested statistically to assess species differentiation. Significant differences were found in 1941 bands ($p < 0.05$), with 477 bands at $p < 0.01$. Spectral separability, measured by the Jeffries-Matusita distance, showed most species could be separated, except for those in the Rhizophoraceae family. Using high-resolution multispectral remote sensing images, the location of species, *A. marina*, *A. alba*, and *A. officinalis* along the gradients of soil salinity were identified by Mitra and Karmaker (2010) having ecological optima at salinity values of 18.2 and 20.1 ppt, 17.5 and 18.6 ppt, and 13.02 and 25 ppt, respectively, indicating *A. marina* as the most salt-tolerant mangrove species in the Indian Sundarbans. Giri et al. (2014) employed Landsat TM and ETM+ images from 2010 and 1999, respectively, to detect changes in particular mangrove species zones, revealing that *Avicennia* sp. is the most dominant species, followed by *Excoecaria* sp. and *Phoenix* sp. Using Landsat satellite series images, Ghosh et al. (2016) were able to identify mangrove species composition and detect species-level over time, showing that *H. fomes* and *E. agallocha* both decreased by 9.9% in the Indian Sundarbans, while *Ceriops decandra*, *Sonneratia apelatala*, and *Xylocarpus mekongensis* increased by 12.9%, 38.4% and 57.3%, respectively.

Recently, a framework was developed using multisource spaceborne high-resolution imagery such as WorldView-2 (WV-2), Orbital HyperSpectral (OHS), and Advanced Land Observing Satellite-2 (ALOS-2) to classify mangrove species at a finer scale. Key variables for species classification were identified through the application of extreme gradient boosting with recursive feature elimination

(XGBoost-RFE) (Zhen et al., 2024). Anand et al. (2020) utilized Hyperion EO-1 hyperspectral satellite data (220 bands) to map dominant species in the Bhitarkanika mangroves through spectral angle mapping (SAM) and partial least squares regression (PLSR). According to the study, *Avicennia marina* had stronger reflectance in SWIR region because of leaf salt excretion, whereas *Rhizophora mucronata* had strong absorption in the NIR region because of its denser canopy structure and indicated overall classification accuracies of 80–85%.

10 Sundarbans Mangrove of India: A Case Study

The Indian Sundarbans, recognised as a World Heritage Site by UNESCO, is a biodiversity hotspot and a unique ecosystem by being the world's largest continuous mangrove ecosystem. This ecosystem plays a key role both ecologically and economically by protecting the area from cyclone-driven coastal erosion and for people's livelihoods by providing resources such as honey, fuelwood, and fish. The climate of the Sundarbans is subtropical. Temperature changes from 20 °C in December–January to 28 °C in June–July. The annual average rainfall is around 1963 mm, 75% of which occurs during June to September. This is in a tropical cyclone belt and often demonstrates a complex interaction between social and ecological systems.

The fluctuating water levels, temperature, and wind flow are affecting the topography of the area, making it prone to several natural hazards, leading to the destruction of forest resources, especially under climate change scenarios. The Sundarbans faces severe climate change challenges, including rising sea levels, increasing salinity, and frequent cyclones, which threaten both its ecosystem and local livelihoods. Some urgent actions, such as global emission reductions, promoting saline-resistant plants, and improving disaster response, are needed to protect the region from further damage and potential submergence (Mahadevia Ghimire & Vikas, 2012). Native mangrove species like *Avicennia marina*, *Rhizophora mucronata*, *Sonneratia apetala*, and *Ceriops decandra* are recognized for their high resistance to salt, ability to adapt to changing water conditions, and importance in stabilizing soil and supporting biodiversity. *Avicennia marina* can tolerate salinity levels over 60 parts per thousand (Parida & Jha, 2010). The forest area of the Sundarbans region is divided into two broad categories: (1) saltwater heritiera and (2) low mangrove. A large part of the 'reserve' forest areas known as 'tiger reserves' has been declared 'totally protected', and no forestry operation is allowed there. The most noted species of the wildlife of the region are the royal Bengal tiger, spotted deer, wild boar, and crocodiles.

The anthropogenic interference in the Sundarbans began in the late eighteenth century mainly through agricultural practices. The deforestation contributes 6–17% of anthropogenic CO_2 emission, for example, from 2000 to 2010, about 1.0 Pg C/year was emitted (Baccini et al., 2012). Further, the encroachment of seawater into the mangrove increases salinity, resulting in loss of high-value storm-stopping tree

species such as Sundari (*Heritiera littoralis*), which gives this area the name Sundarbans. This is further affected by reduced freshwater and sediment supply to the system due to upstream dams on the rivers. There are many indicators of such deleterious effects, e.g. few mangrove islands have vanished over the last century, some have significantly shrunk over the last 50 years, houses are swept away due to repeated collapse of river embankments, abandoning rice farming for shrimping, and increased incidence of water-borne diseases. A comparison of the area with earlier survey records (e.g. early nineteenth-century Dampier and Hodges survey of forest extent) indicates that the mangrove has shrunk to almost half in size.

India's current mangrove cover is 4991.68 km^2, or 0.15% of its entire geographical area. According to the Forest Survey of India, the mangrove cover is categorized into Very Dense (canopy density of 70% and above), Moderately Dense (canopy density of 40% and more but less than 70%) and Open categories (canopy density of 10% and more but less than 40%). Very Dense Mangroves encompass 1463.97 km^2 (29.33% of the total mangrove area); Moderately Dense Mangroves cover 1500.81 km^2 (30.07%); and Open Mangroves cover 2026.87 km^2 (40.60%). India's mangrove cover has decreased from 2021 to 2023 by a net 7.43 km^2. The highest mangrove cover is found in the Sundarbans region of West Bengal (42.5% of the India's total mangrove cover) followed by Gujarat (23.3%), Andhra Pradesh (8.4%), Maharashtra (6.3%), and Odisha (5.2%). West Bengal has the largest expanse of extremely dense mangroves, covering about 981.63 km^2 out of the total mangrove area of 2119.16 km^2 followed by Gujarat, which contains 1164.06 km^2 of mangrove cover, predominantly featuring open mangroves (Table 3). The lowest mangrove cover is found in the Karaikal District of Puducherry. The states that show significant gain in mangrove cover are Andhra Pradesh (13 km^2) and Maharashtra (12 km^2). The rise in mangrove cover in Andhra Pradesh is mostly due to natural regeneration and plantation initiatives, conservation efforts and addition of leftover patches. Andhra Pradesh's districts of Krishna, Bapatla, and Kakinada have all seen a rise. In Maharashtra, the increase in mangrove cover is mostly attributable to natural regeneration and plantations done by the State government. The growth in mangrove cover has been found in the Raigarh and Palghar districts of Maharashtra. But there is a prominent decrease in mangrove cover observed in Gujarat by 36 km^2 (India State of Forest Report, Vol. 1, 2023).

The Land Use Land Cover (LULC) analysis and mapping of the Sundarbans region of the state of West Bengal in India were carried out to provide information to help users understand the problems and prospects of the unique ecosystem. The Landsat data for the years 1988 and 2022 were used for LULC classification using supervised classification in the QGIS environment (Fig. 2). The Sundarbans region was classified into seven LULC classes, such as forest, vegetation, river, water body, fallow land, agricultural land, and built-up areas for both years using a supervised classification method. The respective changes of these classes were −313.8, +139.0, −102.4, +259.0, +625.8, −1465.9, and +858.2 km^2. The positive sign (+) denoted the increase of the area under a particular class, and the negative sign (−) denoted its decrease in the year of 2022 from 1988. Over 34 years of time, the lands under the forest, river, and agriculture classes have decreased substantially. However, the

Table 3 State/Union Territories (UT)-wise Mangrove Cover Assessment 2023 (in km^2) in India

Sl. no.	State/UT	Very dense mangrove	Moderately dense mangrove	Open mangrove	Total mangrove cover
1	Andhra Pradesh	0.00	213.90	207.53	421.43
2	Goa	0.00	23.75	7.59	31.34
3	Gujarat	0.00	179.09	984.97	1164.06
4	Karnataka	0.11	3.15	10.94	14.20
5	Kerala	0.00	4.73	4.72	9.45
6	Maharashtra	0.00	89.82	225.27	315.09
7	Odisha	81.67	94.61	82.78	259.06
8	Tamil Nadu	1.19	25.07	15.65	41.91
9	West Bengal	981.63	703.79	433.74	2119.16
10	A & N Islands	399.37	162.64	46.28	608.29
11	D& NH and Daman & Diu	0.00	0.21	3.65	3.86
12	Puducherry	0.00	0.08	3.75	3.83
Total		**1463.97**	**1500.94**	**2046.87**	**5011.78**

Source: India's Biennial State of Forest Report, 2023

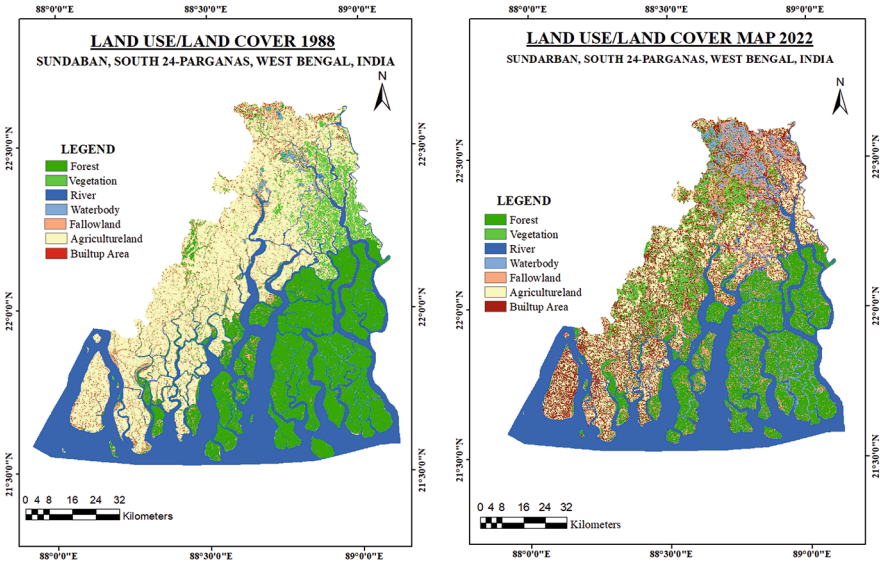

Fig. 2 Land use land cover map of the Indian Sundarbans region for the years 1988 and 2022

lands under other vegetation, water bodies (other than rivers), fallow, and built-up areas have increased in the Sundarbans region. This LULC mapping will enable the monitoring of temporal dynamics of agricultural ecosystems, forest conversions, surface water bodies, etc. on a timely basis for fulfilling the sustainable development goal in the Indian Sundarbans region.

11 Future Need for Remote Sensing Research on Mangrove

Mangrove forests are threatened by many human pressures, including conversion to aquaculture and agriculture, coastal development, overharvesting, agricultural and industrial pollutions, and climate change impacts. There is an urgent need for homogenized classification schemes and standardized data-processing methods for remote sensing-based assessment of mangrove ecosystems using common platforms like Google Earth Engine, Copernicus Global Land Services, etc. This will enable a coherent and seamless data accessibility to the next users for generating the new comparable data with the archive. Similarly, a homogenized transparent accuracy assessment will give confidence for prioritizing the issues. This can provide insights into researchable issues and the adoption of new techniques for the mangrove ecosystems. Developing a database management system for the world mangrove will promote further investigations on synergetic data use. Satellite and unmanned aerial vehicle (UAV) can play a major role in the evaluation of ecosystem services of mangrove by interdisciplinary and well-networked research teams at the regional, national, and global level.

Acknowledgements This chapter is an outcome of the Multinational Collaborative Project partially supported by Asia Pacific Network for Global Change Research (APN-GCR) and University of the Sunshine Coast (UniSC), Australia. The logistic support from the Indian Council of Agricultural Research for the study is duly acknowledged.

References

Anand, A., Pandey, P. C., Petropoulos, G. P., Pavlides, A., Srivastava, P. K., Sharma, J. K., & Malhi, R. K. M. (2020). Use of hyperion for mangrove forest carbon stock assessment in Bhitarkanika forest reserve: A contribution towards blue carbon initiative. *Remote Sensing, 12*(4), 597.

Baccini, A. G. S. J., Goetz, S. J., Walker, W. S., Laporte, N. T., Sun, M., Sulla-Menashe, D., Hackler, J., Beck, P. S. A., Dubayah, R., Friedl, M. A., & Samanta, S. (2012). Estimated carbon dioxide emissions from tropical deforestation improved by carbon-density maps. *Nature Climate Change, 2*(3), 182–185.

Baccini, A., Walker, W., Carvalho, L., Farina, M., Sulla-Menashe, D., & Houghton, R. A. (2017). Tropical forests are a net carbon source based on aboveground measurements of gain and loss. *Science, 358*(6360), 230–234.

Barbier, E. B., Hacker, S. D., Kennedy, C., Koch, E. W., Stier, A. C., & Silliman, B. R. (2011). The value of estuarine and coastal ecosystem services. *Ecological Monographs, 81*(2), 169–193.

Basyuni, M., Mubaraq, A., Amelia, R., Wirasatriya, A., Iryanthony, S. B., Slamet, B., Al Mustaniroh, S. S., Pradisty, N. A., Sidik, F., Hanintyo, R., & Sumarga, E. (2025). Mangrove aboveground biomass estimation using UAV imagery and a constructed height model in Budeng–Perancak, Bali, Indonesia. *Ecological Informatics, 86*, 103037.

Bello, O. M., & Aina, Y. A. (2014). Satellite remote sensing as a tool in disaster management and sustainable development: Towards a synergistic approach. *Procedia-Social and Behavioral Sciences, 120*, 365–373.

Biswas, S., Sarkar, K., & Das, T. K. (2024). Decadal changes (1980–2021) of shoreline and mangrove cover in Sundarban Delta, India, using remote sensing and GIS. *Journal of Physical Oceanography, 54*(8), 1655–1674.

Campomanes, F., Pada, A. V., & Silapan, J. (2016, September). Mangrove classification using support vector machines and random forest algorithm: A comparative study. In *6th International Conference on Geographic Object-Based Image Analysis, GEOBIA 2016: Solutions & Synergies*. University of Twente, Faculty of Geo-Information Science and Earth Observation (ITC).

Castillo, J. A. A., Apan, A. A., Maraseni, T. N., & Salmo, S. G., III. (2017). Estimation and mapping of above-ground biomass of mangrove forests and their replacement land uses in the Philippines using Sentinel imagery. *ISPRS Journal of Photogrammetry and Remote Sensing, 134*, 70–85.

Chapman, V. J. (1976). Mangrove vegetation. J. Cramer, Vaduz, Pp. 447.

Church, J. A., & White, N. J. (2011). Sea-level rise from the late 19th to the early 21st century. *Surveys in Geophysics, 32*(4), 585–602.

Clark, D. A., Piper, S. C., Keeling, C. D., & Clark, D. B. (2003). Tropical rain forest tree growth and atmospheric carbon dynamics linked to interannual temperature variation during 1984–2000. *Proceedings of the National Academy of Sciences, 100*(10), 5852–5857.

Coops, N. C., Wulder, M. A., & White, J. C. (2006). Identifying and describing forest disturbance and spatial pattern: Data selection issues and methodological implications. In *Forest disturbance and spatial pattern: Remote sensing and GIS approaches* (p. 264).

Crowe, M. (2020). Do mangroves burn? A remote sensed study of the impacts of forest fires on mangrove populations in South Sumatra, Indonesia. MSc degree in Climate Change Science and Policy, King's College London.

Datta, D., & Deb, S. (2012). Analysis of coastal land use/land cover changes in the Indian Sunderbans using remotely sensed data. *Geo-spatial Information Science, 15*(4), 241–250.

Dookie, S., Ansari, A. A., & Jaikishun, S. (2025). Forest-fire interactions, impacts, and implications: A focus on mangroves. *New Zealand Journal of Forestry Science, 55*.

Duke, N., Ball, M., & Ellison, J. (1998). Factors influencing biodiversity and distributional gradients in mangroves. *Global Ecology & Biogeography Letters, 7*(1), 27–47.

Dutta, D., Das, P. K., Paul, S., Sharma, J. R., & Dadhwal, V. K. (2015). Assessment of ecological disturbance in the mangrove forest of Sundarbans caused by cyclones using MODIS time-series data (2001–2011). *Natural Hazards, 79*(2), 775–790.

FAO, 2020. Global Forest Resources Assessment 2020: Main report. .

Ganguly, S., Nemani, R. R., Zhang, G., Hashimoto, H., Milesi, C., Michaelis, A., Wang, W., Votava, P., Samanta, A., Melton, F., & Dungan, J. L. (2012). Generating global leaf area index from Landsat: Algorithm formulation and demonstration. *Remote Sensing of Environment, 122*, 185–202.

Ghosh, S., & Mistri, B. (2022). Analyzing the multi-hazard coastal vulnerability of Matla–Bidya inter-estuarine area of Indian Sundarbans using analytical hierarchy process and geospatial techniques. *Estuarine, Coastal and Shelf Science, 279*, 108144.

Ghosh, A., Schmidt, S., Fickert, T., & Nüsser, M. (2015). The Indian Sundarban mangrove forests: History, utilization, conservation strategies and local perception. *Diversity, 7*(2), 149–169.

Ghosh, M. K., Kumar, L., & Roy, C. (2016). Mapping long-term changes in mangrove species composition and distribution in the Sundarbans. *Forests, 7*(12), 305.

Ghosh, S. M., Behera, M. D., Jagadish, B., Das, A. K., & Mishra, D. R. (2021). A novel approach for estimation of aboveground biomass of a carbon-rich mangrove site in India. *Journal of Environmental Management, 292*, 112816.

Gilman, E. L., Ellison, J., Duke, N. C., & Field, C. (2008). Threats to mangroves from climate change and adaptation options: A review. *Aquatic Botany, 89*(2), 237–250.

Giri, C., Pengra, B., Zhu, Z., Singh, A., & Tieszen, L. L. (2007). Monitoring mangrove forest dynamics of the Sundarbans in Bangladesh and India using multi-temporal satellite data from 1973 to 2000. *Estuarine, Coastal and Shelf Science, 73*(1–2), 91–100.

Giri, S., Mukhopadhyay, A., Hazra, S., Mukherjee, S., Roy, D., Ghosh, S., Ghosh, T., & Mitra, D. (2014). A study on abundance and distribution of mangrove species in Indian Sundarban using remote sensing technique. *Journal of Coastal Conservation, 18*(4), 359–367.

Global Mangrove Watch. (2020). *Mangrove extent dataset*. https://www.globalmangrovewatch.org

Gupta, S. (2021). Disturbance of mangrove forest due to climate change: The prospects of Sundarban. *International Journal of Multidisciplinary: Applied Business and Education Research, 2*(12), 1306–1313.

He, B., Lai, T., Fan, H., Wang, W., & Zheng, H. (2007). Comparison of flooding-tolerance in four mangrove species in a diurnal tidal zone in the Beibu Gulf. *Estuarine, Coastal and Shelf Science, 74*(1–2), 254–262.

Healey, S. P., Cohen, W. B., Zhiqiang, Y., & Krankina, O. N. (2005). Comparison of Tasseled Cap-based Landsat data structures for use in forest disturbance detection. *Remote Sensing of Environment, 97*(3), 301–310.

IPCC. (2013). Summary for policymakers. In T. F. Stocker, D. Qin, G.-K. Plattner, M. Tignor, S. K. Allen, J. Boschung, A. Nauels, Y. Xia, V. Bex, & P. M. Midgley (Eds.), *Climate change 2013: The physical science basis. Contribution of Working Group I to the Fifth Assessment Report of the Intergovernmental Panel on Climate Change*. Cambridge University Press.

Iqbal, M. H. (2020). Valuing ecosystem services of Sundarbans Mangrove Forest: Approach of choice experiment. *Global Ecology and Conservation, 24*, e01273.

IUCN. (2025). *The IUCN red list of threatened species*. Version 2025-1. Retrieved July 28, 2025.

Jiang, Y., Zhang, L., Yan, M., Qi, J., Fu, T., Fan, S., & Chen, B. (2021). High-resolution mangrove forests classification with machine learning using worldview and UAV hyperspectral data. *Remote Sensing, 13*(8), 1529.

Jose, S., Alex, C. J. C. J., Kumar, S., Varghese, A., & Madhu, G. (2011). Landscape metric modeling—A technique for forest disturbance assessment in Shendurney wildlife sanctuary. *Environmental Research, Engineering and Management, 58*(4), 34–41.

Kanjin, K., & Alam, B. M. (2024). Assessing changes in land cover, NDVI, and LST in the Sundarbans mangrove forest in Bangladesh and India: A GIS and remote sensing approach. *Remote Sensing Applications: Society and Environment, 36*, 101289.

Kuenzer, C., Bluemel, A., Gebhardt, S., Quoc, T. V., & Dech, S. (2011). Remote sensing of mangrove ecosystems: A review. *Remote Sensing, 3*(5), 878–928.

Kumar, T., Mandal, A., Dutta, D., Nagaraja, R., & Dadhwal, V. K. (2019). Discrimination and classification of mangrove forests using EO-1 Hyperion data: A case study of Indian Sundarbans. *Geocarto International, 34*(4), 415–442.

Kundu, K., Halder, P., & Mandal, J. K. (2021). Change detection and patch analysis of Sundarban forest during 1975–2018 using remote sensing and GIS data. *SN Computer Science, 2*(5), 364.

Kurbanov, E., Vorobev, O., Lezhnin, S., Sha, J., Wang, J., Li, X., Cole, J., Dergunov, D., & Wang, Y. (2022). Remote sensing of forest burnt area, burn severity, and post-fire recovery: A review. *Remote Sensing, 14*(19), 4714.

Mahadevia Ghimire, K., & Vikas, M. (2012). Climate change–impact on the Sundarbans, a case study. *International Scientific Journal: Environmental Science, 2*(1), 7–15.

Mandal, M. S. H., & Hosaka, T. (2020). Assessing cyclone disturbances (1988–2016) in the Sundarbans mangrove forests using Landsat and Google Earth Engine. *Natural Hazards, 102*(1), 133–150.

Mandal, P., Maiti, A., Paul, S., Bhattacharya, S., & Paul, S. (2022). Mapping the multi-hazards risk index for coastal block of Sundarban, India using AHP and machine learning algorithms. *Tropical Cyclone Research and Review, 11*(4), 225.

Mildrexler, D. J., Zhao, M., & Running, S. W. (2009). Testing a MODIS global disturbance index across North America. *Remote Sensing of Environment, 113*(10), 2103–2117.

Mitra, D., & Karmaker, S. (2010). Mangrove classification in Sundarban using high resolution multi-spectral remote sensing data and GIS. *Asian Journal of Environment and Disaster Management, 2*(2).

Mondal, I., & Bandyopadhyay, J. (2014). Coastal zone mapping through geospatial technology for resource management of Indian Sundarban, West Bengal, India. *International Journal of Remote Sensing Applications, 4*(2), 103–112.

Mondal, I., Thakur, S., Ghosh, P., De, T. K., & Bandyopadhyay, J. (2018). Land use/land cover modeling of Sagar Island, India using remote sensing and GIS techniques. In *Emerging technologies in data mining and information security: Proceedings of IEMIS 2018* (Vol. 1, pp. 771–785). Springer Singapore.

Mondal, B. K., Mahata, S., Basu, T., Das, R., Patra, R., Abdelrahman, K., Fnais, M. S., & Praharaj, S. (2024). Analysis of the post-cyclonic physical flood susceptibility and changes of mangrove forest area using multi-criteria decision-making process and geospatial analysis in Indian Sundarbans. *Atmosphere, 15*(4), 432.

Mukherjee, N., Sutherland, W. J., Khan, M. N. I., Berger, U., Schmitz, N., Dahdouh-Guebas, F., & Koedam, N. (2014). Using expert knowledge and modeling to define mangrove composition, functioning, and threats and estimate time frame for recovery. *Ecology and Evolution, 4*(11), 2247–2262.

Nerem, R. S., Chambers, D. P., Choe, C., & Mitchum, G. T. (2010). Estimating mean sea level change from the TOPEX and Jason altimeter missions. *Marine Geodesy, 33*(S1), 435–446.

NOAA. (2015). National Oceanic and Atmospheric Administration, National Ocean Service, Center for Operational Oceanographic Products and Services, Tides and Currents. http://tidesandcurrents.noaa.gov/

NOAA. (2023). *Cyclone hazards & safety*. https://www.noaa.gov/jetstream/tc-hazards

Padhy, S. R., Dash, P. K., & Bhattacharyya, P. (2022). Challenges, opportunities, and climate change adaptation strategies of mangrove-agriculture ecosystem in the Sundarbans, India: A review. *Wetlands Ecology and Management, 30*(1), 191–206.

Parida, A. K., & Jha, B. (2010). Salt tolerance mechanisms in mangroves: A review. *Trees, 24*(2), 199–217.

Parida, B. R., & Kumar, P. (2020). Mapping and dynamic analysis of mangrove forest during 2009–2019 using landsat–5 and sentinel–2 satellite data along Odisha Coast. *Tropical Ecology, 61*(4), 538–549.

Paul, A. K., Ray, R., Kamila, A., & Jana, S. (2017). Mangrove degradation in the Sundarbans. In *Coastal wetlands: Alteration and remediation* (pp. 357–392). Springer International Publishing.

Prakash, S., Varghese, A., Amrutha, A. S., & Baiju, K. R. (2023). Assessment of ecological disturbance on Indian sundarbans with special reference to Amphan Cyclone by using geospatial technology. *Journal of Geospatial Surveying, 3*(1), 26.

Randhir, T. O., Toffling, K., & Griffin, C. R. (2024). Impacts of climate change and variability on the growth potential of global mangrove distribution. *Sustainable and Resilient Infrastructure, 9*(1), 63–71.

Razali, S. M., Nuruddin, A. A., Malek, I. A., & Patah, N. A. (2010). Forest fire hazard rating assessment in peat swamp forest using Landsat thematic mapper image. *Journal of Applied Remote Sensing, 4*(1), 043531.

Salam, M. A., Ross, L. G., & Beveridge, C. M. C. (2007). The use of GIS and remote sensing techniques to classify the Sundarbans Mangrove vegetation. *Journal of Agroforestry and Environment, 1*(1), 7–15.

Samanta, K., & Hazra, S. (2016). Mangrove forest cover changes in Indian Sundarban (1986–2012) using remote sensing and GIS. In *Environment and earth observation: Case studies in India* (pp. 97–108). Springer International Publishing.

SEI (Stockholm Environment Institute). (2023). *NASA data and images help increase climate resilience in the Mekong region*. https://www.sei.org/features/nasa-data-images-help-increase-climate-resilience-mekong-region/

SERVIR Global. (2023). *SERVIR-Mekong*. https://www.servirglobal.net/Global/Regions/SERVIR-Mekong

Shimu, S. A., Aktar, M., Afjal, M. I., Nitu, A. M., Uddin, M. P., & Al Mamun, M. (2019, December). NDVI based change detection in Sundarban Mangrove Forest using remote sensing data. In

2019 4th International Conference on Electrical Information and Communication Technology (EICT) (pp. 1–5). IEEE.

Simard, M., Fatoyinbo, L., Smetanka, C., Rivera-Monroy, V. H., Castañeda-Moya, E., Thomas, N., & Van der Stocken, T. (2019). Mangrove canopy height globally related to precipitation, temperature and cyclone frequency. *Nature Geoscience, 12*(1), 40–45.

Srivastava, S. K., Seng, K. P., Ang, L. M., Pachas, A. N. A., & Lewis, T. (2022). Drone-based environmental monitoring and image processing approaches for resource estimates of private native forest. *Sensors, 22*(20), 7872.

Thakur, S., Maity, D., Mondal, I., Basumatary, G., Ghosh, P. B., Das, P., & De, T. K. (2021). Assessment of changes in land use, land cover, and land surface temperature in the mangrove forest of Sundarbans, northeast coast of India. *Environment, Development and Sustainability, 23*(2), 1917–1943.

Tomlinson, P. B. (2016). *The botany of mangroves*. Cambridge University Press.

UNEP. (2023). *State of the world's mangroves 2023*. United Nations Environment Programme. https://www.unep.org/resources/report/state-worlds-mangroves-2023

Vadrevu, K. P., Eaturu, A., & Badarinath, K. (2010). Fire risk evaluation using multicriteria analysis—A case study. *Environmental Monitoring and Assessment, 166*(1), 223–239.

Vaiphasa, C., Ongsomwang, S., Vaiphasa, T., & Skidmore, A. K. (2005). Tropical mangrove species discrimination using hyperspectral data: A laboratory study. *Estuarine, Coastal and Shelf Science, 65*(1–2), 371–379.

Vyas, P., & Sengupta, K. (2012). Mangrove conservation and restoration in the Indian Sundarbans. In *Sharing lessons on mangrove restoration* (p. 93).

Ward, R. D., Friess, D. A., Day, R. H., & Mackenzie, R. A. (2016). Impacts of climate change on mangrove ecosystems: A region by region overview. *Ecosystem Health and Sustainability, 2*(4), e01211.

Zhen, J., Mao, D., Shen, Z., Zhao, D., Xu, Y., Wang, J., Jia, M., Wang, Z., & Ren, C. (2024). Performance of xgboost ensemble learning algorithm for mangrove species classification with multisource spaceborne remote sensing data. *Journal of Remote Sensing, 4*, 0146.